Journal of Applied Sciences and Nanotechnology

Laser-Induced Breakdown Spectroscopy: Principles and Advanced Applications

Rajaa N. Ketan*, Muayyed J. Zoory, Haidar J. Mohamad

Department of Physics, College of Science, Mustansiriyah University, Iraq

A R T I C L E I N F O

*Corresponding Author:
Rajaa N. Ketan
rajaa.n@csw.uobaghdad.edu.iq

A B S T R A C T

A spectroscopic technique such as laser-induced breakdown spectroscopy (LIBS) is used to analyze various materials, including solids, liquids and gases. The advantages of this technique include rapid analysis, no prior sample preparation, low cost and the ability to generate qualitative and quantitative analytical data for any sample. There are numerous applications for LIBS in various fields, including environmental monitoring, quality in industry, the food sector and archeology, medicine (pharmaceuticals), biology (bones, nails, hair, blood and skin) and cosmetics, which is one of the main concerns of the World Health Organization due to its significant impact on health. In this review, the LIBS technique is explained in terms of the experimental setup (laser, detector, spectrometer, optical fibers and lenses), using single and double beams to measure sample elements with high accuracy. It was shown that the sensitivity of LIBS depends on calibration-free analysis and pulse-coupled analysis. The data show that the double laser beams provide high accuracy when analyzing complex data.

1. Introduction

Laser-Induced Breakdown Spectroscopy (LIBS) is a rapid analytical technique capable of simultaneously identifying the elemental composition of any sample whether in gas, liquid, or solid form both qualitatively and quantitatively [1-3]. The LIBS technique depends on high-energy radiation produced by various types of lasers that emit short pulses. The capability to generate high-energy pulses in Q-switch mode sets these lasers apart. They are stimulated using various optical methods. Solid-state Nd: YAG lasers are extensively employed. The emission sources of these lasers include noble gas or halogen lamps, with a wavelength ranging from 200 to 1000 nm, or lasers with narrow-band semiconductors working at a wavelength of 1064 nm. The pulse durations are within the nanosecond range. The plasma that emits light is generated by the interaction between the laser beam and the surface of the sample. The emitted light is collected by an optical cable and transmitted to a spectrometer, which then generates the spectrum of the sample. Spectral analysis is used to determine the chemical elements in the sample with high precision [4].

The advantages of LIBS in elemental detection and quantification are represented by its simplicity, does not require any sample preparation, and the analysis can be performed without any toxic substances or contaminants. The

obtained spectra are generated rapidly and easily, making LIBS an efficient and eco-friendly choice across various applications and fields [5]. Thus, LIBS is applicable in various applications including a wide range of materials, such as metals, alloys, organic and inorganic substances, as well as biological and medical samples [6, 7] ,to study human tissues and identify chemical changes related to diseases, bones and teeth, determination of drug composition, and perform physiological examination of body fluids such as blood [8].

There are several recent studies proven LIBS as an effective technology in several fields. Forster and Lewis (2018) explored the impact of double laser pulses (DPs) on the ablation process in solid materials by employing a two-thermal hybrid model designed by the combination of a continuum method to conduct band electrons with a dynamics (MD) procedure for ions. To investigate the association between pulses with delays in a range of 0 to 50 lbs and absorbed laser fluences of 0.5, 1.0, and 1.5 J/m², corresponding to 1–3 times the ablation threshold for single-pulse (SP) ablation on aluminum (Al) sample. This study provided an exhaustive knowledge of the process mechanisms during the ablation stages initiated by DPs. The study concluded the improvement of the evaporation in DP ablation, which might improve the accuracy of the emission spectra [9]. Wang *et al*. (2018) used Artificial Neural Networks (ANN), Principal Component Analysis (PCA), and LIBS to investigate and classify three different types of Chinese herbal medicines: Rhizomes Ligusticum Walachia, Codonopsis Pilosula, and Angelica pubescens with various origins or parts. The PCA was employed to create the score matrix. A back-propagation artificial neural network framework was developed to determine the origin of the medication, using the LIBS approach on pubescent roots from three different locations. The findings showed an average classification accuracy of 99.89%, exceeding support vector machine learning and linear discriminant analysis in classification prediction [10]. Malenfant *et al*. (2019) employed the LIBS technology to identify and locate the bacterial cells. A specifically designed centrifugal insert device with two stages was used to achieve rapid sedimentation of bacterial cells via a 0.22 micrometers pore size filter. Subsequently, within 3 minutes 1.5 mL of the obtained suspension was filtered. The results revealed that more than 90% of the bacterial cells in the suspension were successfully identified [11]. Tiwari *et al*. (2020) studied the LIBS potential with statistical methods for analyzing different compositions of drug samples. The study proved the effectiveness of LIBS in distinguishing drug samples with similar elemental compositions. As well as, it is fast, precise and low-cost, which aligns with the requirements of drug analysis [12]. Zhang *et al*. (2021) used the LIBS technique to examine different elements in hair and nail samples as they are vital indicators of dietary status and metabolic changes. LIBBS provide direct collection for the spectral line from the samples. The ratio of Ca/Na and Mg/Na concentration in hair nails was calculated using the reference line method and calibration-free LIBS (CF-LIBS) in the standard. The procedure precision was represented by the results, which indicated that the relative errors among the quantitative results of CF-LIBS and ICPOES were less than 10% in hair and nails. These findings confirmed that the CF-LIBS method is a reliable reference line to be utilized in biological medicine [13]. Sami *et al*. (2024) investigated using the LIBS technique to detect kidney failure in patients suffering from iron deficiency significant statistical differences were observed in the initial blood sample composition compared to healthy individuals. This study proved the benefit of LIBS in the Kidney Health Department [14].

Taraq and Hamad (2024) employed the LIBS technique with a pulsed Nd: YAG laser and a wavelength of 1064 nm, an energy/pulse of 100 mJ, and a pulse width of 9 ns to investigate several dental samples. The spectra of LIBS samples were recorded between 300–600 nm. Analyze the concentrations of elements such as Ca, Mg, C, and Zn in dental samples and compare the obtained results through energy dispersive X-ray (EDX) analysis and inductively coupled plasma mass spectrometry (ICP-MS). ICP-MS demonstrated a higher precision factor (R^2) compared to EDX, reflecting more reliable measurements. However, the inherited properties of the structural and compositional parameters of teeth present challenges for achieving consistent and accurate results with LIBS. Accurate quantitative analysis using standard calibration curves is particularly challenging due to the scarcity of matrix-match reference samples. As a result, there were distinguished differences in the plasma features between dental samples and laboratory-prepared reference materials, further complicating the analysis [15]. Khomeini *et al*. (2024) have used orthogonal double-pulsed laser spectroscopy (DP-LIBS) to accurately and sensitively determine the elemental composition of human blood serum. The elements in serums taken from human blood were examined in a helium gas environment. To activate the luminescent gas plasma, a nucleus pulse of the Nd: YAG laser (1064 nm, 7 ns) was irradiated directly above the target material in an experiment. The material was then exposed to a third harmonic pulse of the Nd: YAG laser (355 nm, 7 ns) to create a target plasma that will

remove atoms from the blood serum film and deliver them to the gas plasma region. It was successfully demonstrated that its LIBS signal strength can be increased up to eight times using the dual pulse LIBS approach. DP-LIBS enabled the accurate identification of many emission lines that were barely noticeable using single-pulse LIBS. Several components of human blood serum were subjected to qualitative and quantitative analysis. The concentrations of C, Ca, K, Mg, Na, Fe, and P in human blood were 8360, 219, 581, 785, 343, 293, and 12 (ppm), respectively. The LIBS data is consistent with those obtained from conventional XRF [16]. The current review will provide the major contribution of LIBS in analyzing various sample types and offer important insights on the comparison between single-beam and dual-beam laser setups to improve the detection sensitivity of characteristic elements. Additionally, it explores developed data analysis methods, including calibration-free approaches, and highlights the versatility of LIBS in medical and biological sciences. As well as discussed, the recent advancements of LIBS to improve its accuracy and efficiency and have presented the growing potential across diverse applications.

2. Theoretical

Compared to traditional methods, LIBS is an adaptable technique to evaluate the composition elements of many types of materials across various applications. However, there are some limitations, including the potential of sample damage during analysis. The most used design for LIBS is the Single Pulse LIBS (SP-LIBS), which is a powerful and inherently destructive plasma generation method, however, might damage the sample during analysis. New procedures have been recently developed for the property's improvement of LIBS. Two highly promising strategies with significant potential to enhance the characteristics of LIBS are CF-LIBS approaches and LIBS with a DP-LIBS [17].

2.1 Calibration-Free LIBS (CF - LIBS)

This technique is one of the approaches employed for quantitative analysis. Lately, its use has increased in quantitative analysis, as it is considered a practical and quick means for determining the elemental structure of an unspecified sample. That method uses shorter laser pulses because it reduces fragmentation, which is an important factor for this method. The effectiveness of this approach relies only on substantive theoretical models that can explain these effects and allow precise applications where the ablation process changes the relative composition of the substances being analyzed in the plasma [18]. Each of the spectral lines is represented visually as A spot within the plane of Boltzmann. The x coordinate indicates a higher level of energy that is involved in the radiative transfer, and the y synchronize represents the line intensity. The Boltzmann plot applies to fitting lines associated with a particular element, such as Fe I lines. The slope of the line in this diagram shows a clear correlation with the temperature of the plasma. The axis value of the linear regression obtained can be directly related to the element concentration. Fig. 1 shows an example of a Boltzmann diagram in which the black and blue numbers represent numerical data for Fe and Cr respectively.
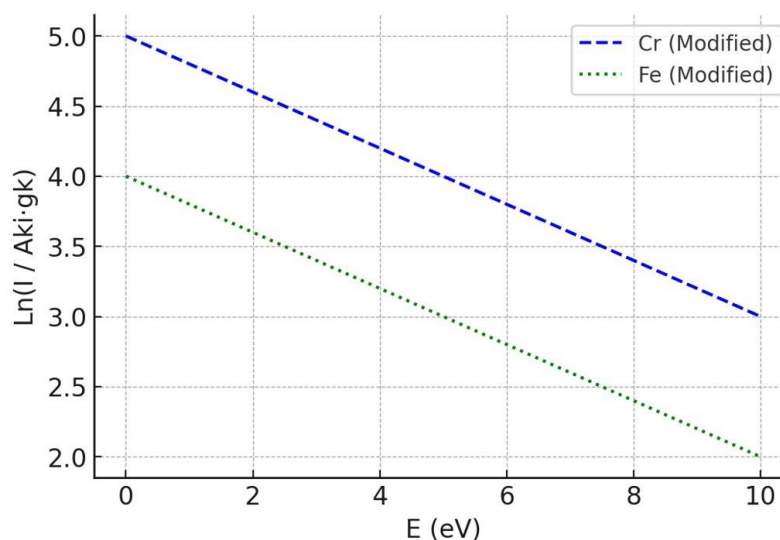
Figure 1: CF - LIBS is based on Boltzmann plot analysis [17].

The CF-LIBS approach relies on the subsequent expectations [19]:

The plasma produced by a laser should be in local Thermodynamic Equilibrium (LTE).

- Ideal transparency is required for plasma.
- A source that is consistently distributed can be used to depict plasma.
- The observable lines of the target from each component are considered when measuring the spectral range.

Concerning spatially thin plasmas under LTE circumstances, the excited levels are populated following the Boltzmann distribution, whereas the states of ionization follow the equilibrium equation of Boltzmann-Saha. For those circumstances, the combined intensity of the line, considering energy transitions and Ei could be expressed in Eq. (1) [20] :

$$I_\lambda^{ki} = FC_s A_{Ki} \frac{g_k e^{-(\frac{Ek}{K_B T})}}{U_s(T)} \qquad (1)$$

Where F is the parameter of the experiment, which includes the density and efficiency of the optical collection plasma, and λ is the measurement of the wavelength of the transition. The variables representing the concentration of the emitting atoms are C_s, the probability of the transition is Aki, the degeneracy level is g_k, the Boltzmann constant is K_B, the temperature of the plasma is T, and the task of the temperature distribution of the emitting species in the plasma is $U_s(T)$. By applying the following changes to the variables in equations (2), (3), (4) and (5) [17] :

$$y = ln\left(\frac{I_\lambda^{ki}}{g_k A_{ki}}\right) \qquad (2)$$

$$m = -\frac{1}{k_B T} \qquad (3)$$

$$q_s = ln\left(\frac{C_S F}{U_S(T)}\right) \qquad (4)$$

The use of the qs parameter, which has a direct relationship to the concentration in the plasma of the species, makes CF-LIBS unique. By finding the intercept (q_s) of the linear regression in the Boltzmann plane, one can calculate the concentration of each species and obtain C_s in equation (5):

$$Cs = \frac{Us(T)}{F} e^{q_s} \qquad (5)$$

where F is the potential factor obtained by normalizing the total concentration of all species.

Singh *et al*. employed the CF-LIBS technique to define the concentration of main and insignificant components in a group of gallstones classified into 3 unique categories (cholesterol stones, mixed stones, and black pigment stones). This analysis aims to identify any possible connections between their composition and possible changes in production mechanisms. Similar to their previous study, the researchers found that different kinds of stones had varying quantities of trace elements also within different sections of a single stone [21].

2.2 Plasma

Plasma is a state of matter, and it has properties and parameters that distinguish it from other states of matter [22-25]:

- Degree of plasma ionization
- Plasma temperature
- Electron density
- Kinetic energy of electrons in plasma
- Thermal velocity of electrons
- Relaxation time of plasma

Equations for particle densities, momenta, and energies can be employed to describe the state of plasma where electron energies reach 0.25–1 eV just a few nanoseconds after laser beam irradiation begins. As a result of collisional ionization processes, 10^{16}–10^{18} cm^3 of electron density are produced. The wavelength determines how strongly the vapors, and the plasma of the developing material absorb the laser light. The absorption coefficient can be calculated using Maxwell's equations (6), (7) and (8) [26] :

$$\alpha = 2k\sqrt{\frac{1}{2}\left\{\sqrt{\left[1-\left(\frac{\omega_p}{\omega}\right)^2\frac{1}{1+\left(\frac{v}{\omega}\right)^2}\right]^2 + \left[\frac{v}{\omega}\left(\frac{\omega_p}{\omega}\right)^2\frac{1}{1+\left(\frac{v}{\omega}\right)^2}\right]^2} - \left[1-\left(\frac{\omega_p}{\omega}\right)^2 - \frac{1}{1+\left(\frac{v}{\omega}\right)}\right]\right\}} \qquad (6)$$

Where c, ω, v, ω_p and α are the vacuum light speed, the laser radiation frequency, the frequency at which electrons collide with ions and atoms, the plasma frequency and the absorption coefficient, respectively. $k = \omega/c$, k is the wave vector in a vacuum. The plasma frequency is the distinctive eigenfrequency of the plasma that describes the oscillation of the electrons for the ions.

$$\omega_p = \sqrt{n_e e^2 / \varepsilon_0 m_e} \qquad (7)$$

where m_e is the electron mass, $\mathcal{E}_0$ is the vacuum permittivity, e is the elementary charge, and n_e is the electron density.

Considering the facts that are distinctive for a laser-induced plasma for LIBS allows for the simplification of Eq. (6) by making the following assumptions $v << \omega$ and $\omega_p < \omega$. For the absorption coefficient Eq. (8):

$$\alpha = \frac{v}{c}\frac{\omega_p^2}{\omega^2\sqrt{1-\left(\frac{\omega_p}{\omega}\right)^2}} \qquad (8)$$

The absorption coefficient is both proportionate to the collision frequency and inversely proportional to the square of the laser light frequency. There are two terms in the collision frequency v_{ei}, v_{en}, where v_{ei} is electrons collision frequency with ions, and v_{en} is the frequency at which electrons collide with atoms. The electron-ion collision frequency is given by Eq. (9) and (10) [27] :

$$v_{ei} = \frac{1}{(4\pi\varepsilon_0)^2}\frac{4\sqrt{2\pi}\ Z^2 e^4 n_i\ ln\Lambda}{3\sqrt{m_e}(k_B T_e)^{3/2}} \qquad (9)$$

where k_B is the constant known as Boltzmann, T_e is the electron temperature, $ln\ \Lambda$ is the logarithm of Coulomb and it is given by Eq. (10):

$$ln\Lambda = ln\left[12\pi\varepsilon_0^{3/2}\frac{(k_B T_e)^{3/2}}{e^3\sqrt{n_e}}\right] \qquad (10)$$

The absorption coefficient as a function of electron density is displayed in Fig. 2. The temperature provided range is seen in LIBS plasma when using Boltzmann plots to measure temperature.
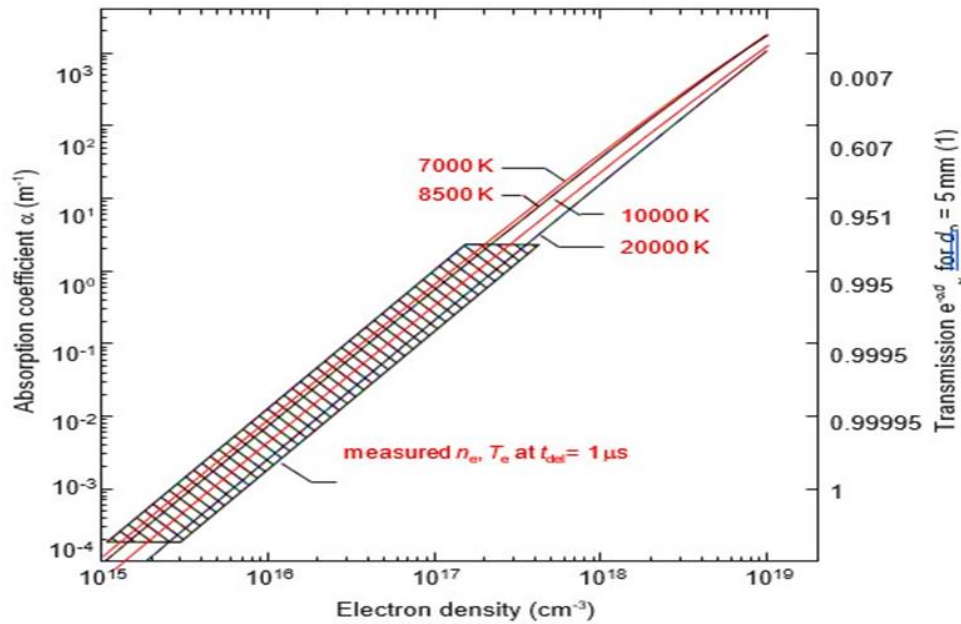
Figure 2: Temperatures of LIBS plasma using Boltzmann diagrams [28].

3. Experimental Details of LIBS

LIBS uses a fast laser pulse directed at a predetermined target. The concentrated energy melts part of the sample. As a result, the laser pulse and the vapor plume interact and create a high-temperature plasma. The light is collected by an optical element (lens or glass fiber) and scattered by a spectrometer. The light comes from the heated atoms and ions in the plasma, which vaporize independently of each other [29].

3.1 Energy Source

The laser source is a crucial component of the LIBS system. Various forms of lasers are utilized for LIBS techniques as well as investigations on ablation. The most used form of laser is the flashlamp-pumped solid-state laser, which utilizes Nd: YAG as the laser [30] a medium was utilized in Q-switching to produce pulses of laser with high intensity and nanosecond pulse lengths. The laser medium is optically stimulated using a wide range of frequencies. Lamps use noble gases or halogens to emit light in the range of 200–1000 nm of the wavelength. The laser possesses high-intensity energy and is eco-friendly with low cost-effectiveness compared with alternative laser options.

3.1.1 Single-Pulse LIBS (SP- LIBS)

Fig. 3 provides an illustrative depiction of a standard experimental setup for LIBS. Required components include a laser that emits short bursts of light, optical devices for concentrating and capturing light, a device for analyzing the light called a spectrometer, and a container for holding the sample. Due to the laser pulse and sample interaction, it removes a small portion of the material, resulting in bright plasma generation. In this plasma, the elements are excited and subsequently return to their original state. The plasma plume then expands and condenses. Subsequently, it results in the generation of electromagnetic radiation that carries specific information about each species found in the sample. Subsequently, the emitted light is sent to the spectrometer by fibre optics. Ultimately, the system software has successfully created a spectral fingerprint. The collimating lens deflects this radiation towards a diffraction grating positioned at a 45° angle with a field of vision perpendicular to the growth of the plasma. Data is gathered from plasma emissions, which generate intensity data [31].
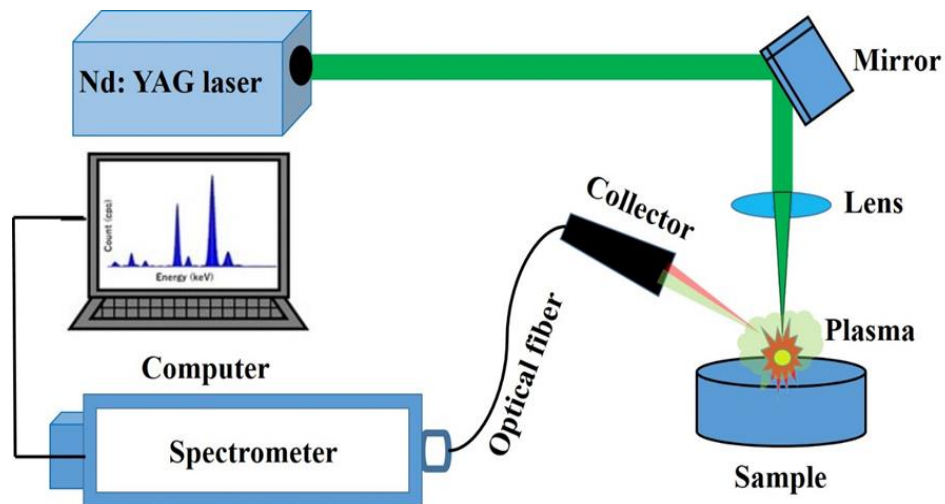
Figure 3: SP- LIBS experimental setup

3.1.2 Double-Pulse LIBS (DP-LIBS)

DP-LIBS technique employed for enhancing the analytical abilities of LIBS for identifying emission lines. It is employed to mitigate the limitations of LIBS by minimizing sample damage. DP-LIBS relies on the use of two consecutive pulses. The first pulse is directed towards the sample, whereas the next pulse is a probe one. This probe pulse is configured to be orthogonal to the first pulse and temporally delayed by it (known as pulse delay time) Fig. 4 Illustrates the three primary configurations of DP-LIBS, collinear orthogonal, pre-ablative, and orthogonal warming configurations, in graphic form [32].

Uebbing (1991) used two laser pulses with wavelengths of 1064 nm and energy levels of 13 mJ and 115 mJ. An unexpected phenomenon occurred when a secondary pulse was directed perpendicular to the sample. This secondary pulse heated the laser-induced plasma. With an energy of 115 mJ and the same wavelength of 1064 nm, the second laser pulse was aligned parallel to the surface of the sample and interacted with the plasma generated by the first pulse 1.5 mm above the surface of the sample. The second pulse has a profound effect on the plasma, raising its temperature to about 6000–10,000 K, resulting in a tenfold increase in the signal intensity of Zn and Cu in the brass sample. However, the volume of the ablated material does not increase [7]. Céline *et al.* (2004) explored the aluminum sample features under atmospheric pressure by employing SP-LIBS and DP-LIBS. In addition, they investigated the time travel impacts between two laser pulses, which were emitted at a wavelength of 532 nm [33], and the samples were ablated at a total energy of 110 mJ. The plasma was reheated by a laser pulse with an energy of 110 mJ and a wavelength of 1064 nm and employing a monochromator and a focal length lens of 100 mm. The gate width (t_w) and gate delay time (td) were set at 4 μs and 3 μs, respectively. To prevent the self-absorption of line emissions, a specially developed aluminum sample containing trace elements was utilized. At the gate delay time (td), the neutral line emission of Mg at 285.21 nm decreased, while the ionic line emissions of Mg (279.55 and 280.27 nm) and Al (281.62 nm) exhibited significant increases in intensity. The application of the second pulse significantly improved detection limits, enhancing them by two to three times, particularly when calibration curves were constructed using ionic lines. This study revealed that the double-pulse reheating approach demonstrated superior sensitivity for ion-emitting components compared to a single-pulse reheating system [34].
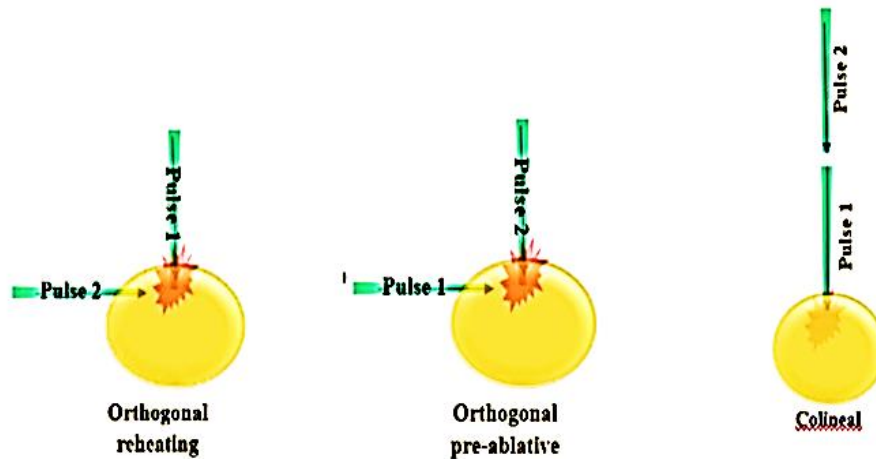
Figure 4: Double Pulse LIBS configurations [17, 35].

3.2 Optical Element (Lens)

The lens captures the laser beam as it leaves the source and directs it onto the target sample for excitation. A higher sample concentration reduces the energy required to extract and remove particles. The photons are then directed to lenses that collect and focus them into an optical fiber system. This optical fiber is equipped with a spherical lens that is coated with an anti-reflective coating to efficiently collect and transmit the photons to the spectrometer [36].

3.3 Plasma Plume

The plasma beam generated by the interaction of the laser with the sample surface expands for about one microsecond. During this time, the atoms in the plasma relax, change from higher to lower orbits and release photons that form the emission spectrum [37].

3.4 Optical Fiber

The use of optical fibers for the transmission of light over long distances is extremely effective. Recent advances in optical fiber materials have made it possible to concentrate power densities of up to megawatts per square centimeter at the end of the fiber without damaging it, allowing tens of millijoules of energy to be transmitted through the fiber. By integrating a lens system at the other end of the fiber, the emitted light can be efficiently focused. To effectively capture the emissions from the plasma, the optical fiber should be only a few millimeters away from the plasma column. The collection angle at the end of the optical fiber makes it possible to capture the light from a large part of the plasma column. Optical fiber bundles have been proposed to simultaneously capture spectral emissions from different areas of the plasma column, facilitating the analysis of specific elements. The use of a single optical fiber for transmitting the laser pulse and capturing the plasma emissions makes the LIBS system ideal for examining samples over longer distances, which is an excellent feature for industrial applications. These fibers can transmit laser pulses over distances of up to 100 meters, with the plasma light being collected and sent back to the detector either via the same fiber or an additional fiber optic cable [38].

3.5 Detector and Spectrometer

A spectrometer is a device used to diffract light emitted from plasma. It consists of an entrance slit, two mirrors, and a diffraction grating. Light enters through the slit and strikes the first mirror, which collides with the light and directs it toward the grating. The diffraction grating reflects the light at various angles relying on its wavelength. The second mirror focuses the light on the detector. Different types of detectors are used in LIBS depending on the practical applications. If the required information is two-dimensional, the most used devices are charge-coupled CCDs and ICCDs. CCD detectors provide a lower background signal, while ICCD detectors provide an improved signal-to-noise ratio (SNR), rapid response times in the nanosecond range, and broad detection capabilities extending from the visible to the infrared spectrum. However, ICCDs are significantly more expensive

than CCDs [29]. The primary spectrometer types employed for LIBS analysis are (a) Turner-Czerny, (b) Echelle, and (c) Paschen-Runge. Fig. 5 shows the configuration of the Eschel spectrometer.
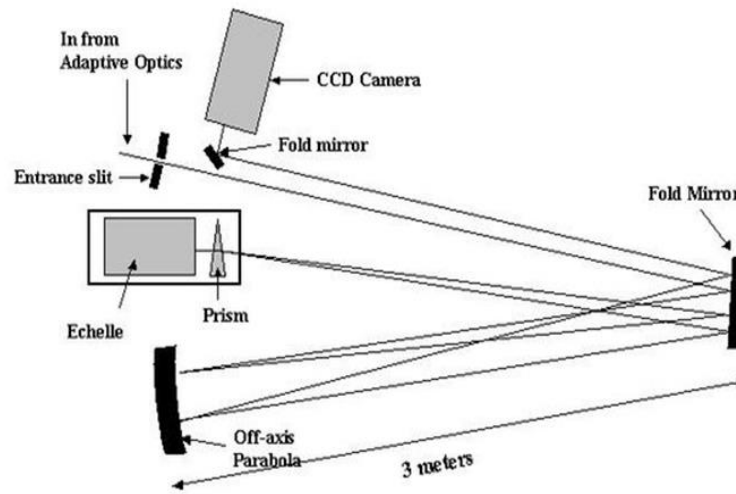
Figure 5. Configuration of the echelle spectroscope apparatus [39].

Table 1 shows the double pulse method, and the corresponding improvements achieved. The double-pulse tests were conducted with substantial alterations in energy, laser type, pulse delay, and laser geometric placement. The enhancements observed, particularly for aluminum (Al), range from 2-fold to as high as 100-fold. The double-pulse technique stands out as the most effective configuration for significantly improving LIBS sensitivity.

Table 1: The utilization of the double-pulse method and its enhancements

Configuration of Beams	Element	No. of Laser	wavelength (nm)	Energy (mJ)	Δt (μs)	improvement	References
Collinear beams	B	2 Nd: YAG	1064	30-76,125	18	15	[40]
	Fe	1 Nd: YAG	1064	80	6	2	[41]
	Mg	2 Nd: YAG	532	140	2.5	3	[42]
	Al	2 Nd: YAG	266,1064	35	3	100	[43]
Orthogonal beams	Cu	2 Nd: YAG	1064	13	40	10	[44]
	Zn	2 Nd: YAG	1064	115	40	10	
Angle of 30	Pb	Ar: F	193	18	1.5	15	[45]

The DP-LIBS technique is one of the most effective methods for enhancing LIBS signals and is widely utilized across various fields. In this procedure, the addition of a laser pulse is influenced by geometric configurations, parameters, and experimental conditions, which are crucial for achieving optimal results. DP-LIBS can also be integrated with spectroscopic analysis, optimization techniques, and other complementary methods. Its applications span diverse industries, including mineral processing, geological exploration, environmental monitoring, biological studies, and various other fields.

4. Results and Discussion

In the past years, there was no usage of LIBS in biomedicine fields, however, recent years witnessed a notable advancement in the applications of LIBS in this biomedicine. LIBS was used to analyze the chemical compositions of human fluids, tissues and bones, which offer novel methods in medical diagnostics and research [49, 50]. Moto-Ross's (2017, 2018) analysis of paraffin-embedded samples and mapping its elements distribution precisely utilized LIBS to map the distribution of elements in paraffin-embedded samples with high precision. The study presented a successful quantification of the elements including phosphorus, calcium, magnesium, zinc, and iron. In specific applications, aluminum and sodium were identified in healthy skin tissue, titanium and phosphorus in cutaneous granulomas and cutaneous pseudolymphoma, phosphorus and titanium in pigmented lymph nodes, and phosphorus, titanium, copper, and chromium in cutaneous scars [46, 47]. These findings provide clear evidence of the capability of LIBS to accurately detect and map elemental distributions in complex biological tissues, making it a valuable tool for biomedical diagnostics and research.

Han *et al.* [48] LIBS was employed to distinguish between skin lesions and adjacent healthy tissue, particularly focusing on melanoma—an aggressive and often asymptomatic form of skin cancer. In this study, melanoma implants were embedded into pressed pellets and analyzed alongside healthy and malignant dermal tissues from mice. Direct spectral examination demonstrated that Principal Component Analysis (PCA) and Linear Discriminant Analysis (LDA) achieved nearly 100% sensitivity and specificity for data reduction and tissue classification, respectively. Multivariate analysis further revealed elevated levels of magnesium and calcium in melanoma tissues.

Dlbyendu and Cheng 2008 aerosolized drugs using (LIBS). The study demonstrates the effectiveness of LIBS as a reliable analytical method for real-time online examination of aerosolized medications. By applying a quantitative LIBS methodology with internal calibration, the spectral data analysis provided accurate measurements of the carbon-to-trace elements (Mg, Fe, and Ca) ratio in three powdered medications: L-Ascorbic Acid (L-AA), Iron L-Ascorbate (ILA), and DL-Pantothenic Acid (DLP). The calculated elemental ratios for carbon-to-magnesium (C/Mg), carbon-to-iron (C/Fe), and carbon-to-calcium (C/Ca) were 4.02 ± 0.76, 12.42 ± 2.36, and 18.47 ± 4.39, respectively. These results closely matched the expected stoichiometric ratios of 4, 12, and 18 based on the chemical compositions of the medications. The findings, summarized in Table 2, confirm the potential of LIBS for precise, real-time analysis of aerosolized pharmaceuticals. Lines of Mg I were collected, and the linear Boltzmann plasma excitation temperatures (T_{exc}) were determined. These temperatures were calculated using time delays of 3.5 μs and 10 μs, as the Mg I lines were distributed across a broad energy range. The linear regressions applied to the corresponding Boltzmann diagrams, generated at delay times of 3.5 μs and 10 μs, respectively. These regressions had coefficients of determination (R^2) of 0.84 and 0.98. From the linear fits ($1/T_{exc}$) slopes at the 3.5 μs and 10 μs delay gates, the estimated plasma excitation temperatures (T_{exc}) were determined to be 6076 - 1102 K and 5263 -284 K, respectively.

Table 2: The overall findings show the ratios of stoichiometric that are anticipated and the likely ratios obtained from LIBS analysis for the elements Ca to C ratio and Ca to Fe ratio, in each of the 3 powdered medicines.

Medicines	Expected C/x ratio	Estimate c/x ratio
L-Ascorbic Acid (Magnesium based L-AA)	4	4.02± 0.76
	4	4.20± 0.79
ILA (iron L-ascorbate; based on Fe)	12	12.42 ± 2.36
DL-Pantothenic Acid (DLP with a Ca basis)	18	18.47±4.39

Table 3 summarizes key studies on the application of LIBS for analyzing biological samples such as bones, nails, and blood, demonstrating its effectiveness in determining elemental compositions with high accuracy.

Table 3: The analysis of biological samples using LIBS

Sample	Researcher	Results	References
Bone	Kasem *el at*.	They used two wavelengths 266 and 1064 nm. The analytical findings demonstrated that LIBS provides an accurate representation of the composition of bone components. Furthermore, bone ash was identified as a suitable standard material for calibrating bone samples in UV-LIBS analysis.	[49]
Nails	Martinez and Baudelet	A film was created by combining alginic acid and keratin with zinc oxide nanoparticles, followed by drying and cross-linking to form a solid surface. The calibration curve achieved a determination coefficient of 0.986, with a Zn detection limit of 13 $\mu g \cdot g^{-1}$ and a quantitation limit of 27 $\mu g \cdot g^{-1}$. Zinc concentrations in two toenail samples were measured using this calibration curve, with accuracy confirmed through bulk ICP-MS analysis. The study demonstrated that LIBS, with custom matrix-matched reference materials, can precisely measure zinc concentrations in fingernails.	[50]
Hair	Hamzaoui *et al.*	Hair samples from individuals with androgenetic alopecia were analyzed for mineral and trace element concentrations, including magnesium (Mg), calcium (Ca), sodium (Na), and potassium (K). Plasma plumes from the parietal and occipital hair regions of 12 subjects were examined for K, Ca, Mg, and Na emission line intensities. Results showed no consistent behavior for Mg intensities, while Ca and Na emission lines were stronger in the occipital region compared to the parietal region.	[51]
Blood	Feng *et al.*	In this study, a portable laser device using LIBS was developed for the rapid and accurate determination of serum electrolytes (K, Na and Ca), which are essential for the diagnosis and prevention of disease. Serum samples were analyzed in real time on filter paper and glass slides. Partial least squares regression (PLSR) was used to determine electrolyte levels based on LIBS spectra and showed high linearity and predictive accuracy. On glass slides, the prediction accuracy was 1.45% (K), 0.61% (Na) and 3.80% (Ca), while the accuracy on filter paper was 7.47% (K), 1.56% (Na) and 0.52% (Ca). The results confirm that the portable LIBS with PLSR enables precise serum analysis in real time, making it very suitable for clinical applications.	[52]
Skin	Qing Sun *et al.*	LIBS was used to evaluate the efficacy of barrier creams in reducing zinc ion uptake by human skin. A Nd:YAG laser (1064 nm, 100 mJ) was used to analyze the penetration of zinc from a lipophilic oil paste (ZnO) and a hydrophilic solution ($ZnCl_2$). The study focused on zinc absorption in the stratum corneum and examined three commercial barrier creams in six participants with skin biopsies taken 0.5 and 3 hours after application. The atomic emission line of zinc (213.9 nm) was analyzed, optimizing the gate delay and width for improved SNR and accuracy. The results showed that the barrier creams were effective in preventing the penetration of zinc ions and ZnO.	[53]

5. Conclusions

The LIBS technique is used in various fields, including biology. It is well on its way to becoming the most effective technique for two analytical methods, qualitative and quantitative. Medical and biological samples are essential for the treatment of diseases that can affect a living organism. Therefore, this review focuses on the analysis of sample elements using this technique. This method works effectively in all states of matter but has some disadvantages, such as limited resolution and possible damage to the sample. However, the double pulse technique has been shown to minimize these problems and increase the sensitivity of LIBS without damaging the sample. Therefore, LIBS is well on its way to becoming one of the most effective methods for quantitative and qualitative analysis.

Author Contribution Statement
All authors contributed equally to this paper.

Conflict of Interest
The authors declare that they have no conflict of interest.

References
[1] B. Busser, S. Moncayo, J.-L. Coll, L. Sancey, and V. Motto-Ros, "Elemental imaging using laser-induced breakdown spectroscopy: A new and promising approach for biological and medical applications," *Coordination Chemistry Reviews,* vol. 358, pp. 70-79, 2018.

[2] Z. J. Kamil, M. J. Zoory, and H. J. Mohamad, "LIBS technique for plant mineral ratio analysis and environmental and agricultural importance: a comprehensive review," *The European Physical Journal D,* vol. 78, no. 3, p. 27, 2024.

[3] R. Nader, H. J. Mohamad, and M. J. Zoory, "Comparison of heavy metals concentrations in toothpaste using atomic absorption analysis and laser-induced breakdown," *Journal of Optics,* pp. 1-8, 2024.

[4] S. Buckley, "LIBS basics, Part I: measurement physics and implementation," 2014.

[5] S. Musazzi and U. Perini, "Laser-induced breakdown spectroscopy," *Springer Series in Optical Sciences,* vol. 182, 2014.

[6] C. Durrant *et al.*, "Ferromagnetic resonance of patterned chromium dioxide thin films grown by selective area chemical vapour deposition," *Journal of Applied Physics,* vol. 117, no. 17, 2015.

[7] D. Mukherjee and M.-D. Cheng, "Characterization of carbon-containing aerosolized drugs using laser-induced breakdown spectroscopy," *Applied spectroscopy,* vol. 62, no. 5, pp. 554-562, 2008.

[8] B. B. S. Jaswal and V. K. Singh, "Analytical assessments of gallstones and urinary stones: a comprehensive review of the development from laser to LIBS," *Applied Spectroscopy Reviews,* vol. 50, no. 6, pp. 473-498, 2015.

[9] G. Förster and L. J. Lewis, "Numerical study of double-pulse laser ablation of Al," *Physical Review B,* vol. 97, no. 22, p. 224301, 2018.

[10] J. Wang, X. Liao, P. Zheng, S. Xue, and R. Peng, "Classification of Chinese herbal medicine by laser-induced breakdown spectroscopy with principal component analysis and artificial neural network," *Analytical letters,* vol. 51, no. 4, pp. 575-586, 2018.

[11] D. J. Malenfant, A. E. Paulick, and S. J. Rehse, "A simple and efficient centrifugation filtration method for bacterial concentration and isolation prior to testing liquid specimens with laser-induced breakdown spectroscopy," *Spectrochimica Acta Part B: Atomic Spectroscopy,* vol. 158, p. 105629, 2019.

[12] P. K. Tiwari, P. K. Rai, and A. K. Rai, "Applications of LIBS in drug analysis," in *Laser-Induced Breakdown Spectroscopy*: Elsevier, 2020, pp. 311-328.

[13] S. Zhang *et al.*, "Quantitative analysis of mineral elements in hair and nails using calibration-free laser-induced breakdown spectroscopy," *Optik,* vol. 242, p. 167067, 2021.

[14] I. Sami, M. J. Zoory, and S. H. Lefta, "Implementation of laser-induced breakdown spectroscopy (LIBS) technique in evaluating of renal failure in patients with iron (Fe) deficiency," *Advancements Life Sci.,* vol. 11, no. 1, pp. 66-77, 2024.

[15] M. S. Tareq and T. K. Hamad, "Quantitative analysis of human teeth by using LIBS technology with different calibration methods: in vitro study," *Journal of Optics,* pp. 1-11, 2024.

[16] A. Khumaeni, W. S. Budi, R. Hedwig, M. A. Gondal, and K. H. Kurniawan, "Signal intensity augmentation of elements detected in blood serum using dual pulse laser induced plasma spectroscopy under ambient he gas environment," *Arabian Journal for Science and Engineering,* vol. 49, no. 1, pp. 1297-1308, 2024.

[17] V. Loera, "Double-Pulse and Calibration-Free Laser-Induced Breakdown Spectroscopy (LIBS) on quantitative analysis," *Doctor of Philosophy, Centro de Investigaciones en Óptica AC, Spain,* 2013.

[18] E. Tognoni, G. Cristoforetti, S. Legnaioli, and V. Palleschi, "Calibration-free laser-induced breakdown spectroscopy: state of the art," *Spectrochimica Acta Part B: Atomic Spectroscopy,* vol. 65, no. 1, pp. 1-14, 2010.

[19] G. Bilge, B. Sezer, K. E. Eseller, H. Berberoglu, A. Topcu, and I. H. Boyaci, "Determination of whey adulteration in milk powder by using laser induced breakdown spectroscopy," *Food chemistry,* vol. 212,

pp. 183-188, 2016.

[20] J. Aguilera and C. Aragón, "Multi-element Saha–Boltzmann and Boltzmann plots in laser-induced plasmas," *Spectrochimica Acta Part B: Atomic Spectroscopy,* vol. 62, no. 4, pp. 378-385, 2007.

[21] V. K. Singh, V. Singh, A. K. Rai, S. N. Thakur, P. K. Rai, and J. P. Singh, "Quantitative analysis of gallstones using laser-induced breakdown spectroscopy," *Applied Optics,* vol. 47, no. 31, pp. G38-G47, 2008.

[22] R. Noll and R. Noll, *Laser-induced breakdown spectroscopy*. Springer, 2012.

[23] M. A. Khater, "Spectroscopic investigations of laser-produced steel plasmas in the vacuum ultraviolet," Dublin City University, 2001.

[24] A. P. Delserieys, "Optical diagnostics of laser plasmas," Queen's University, Belfast, 2008.

[25] G. K. Parks, *Physics of space plasmas: an introduction*. CRC Press, 2019.

[26] A. W. Miziolek, V. Palleschi, and I. Schechter, *Laser induced breakdown spectroscopy*. Cambridge university press, 2006.

[27] A. Anders, *A formulary for plasma physics*. Andre Anders, 1990.

[28] S. Musazzi and U. Perini, "Laser-Induced Breakdown Spectroscopy—Fundamentals and Applications," *Springer Series in Optical Sciences,* 2014.

[29] A. N. Williams, *Measurement of rare earth and uranium elements using laser-induced breakdown spectroscopy (LIBS) in an aerosol system for nuclear safeguards applications*. Virginia Commonwealth University, 2016.

[30] R. Nader, S. I. Ibrahim, and H. M. Yaseen, "Study the effect of changing aperture size on linear and nonlinear properties of wheat germ oil," in *IOP Conference Series: Materials Science and Engineering*, 2020, vol. 928, no. 7: IOP Publishing, p. 072087.

[31] M. Markiewicz-Keszycka *et al.*, "Laser-induced breakdown spectroscopy (LIBS) for food analysis: A review," *Trends in food science & technology,* vol. 65, pp. 80-93, 2017.

[32] S. Buckley, "LIBS basics, Part I: measurement physics and implementation," *Spectroscopy,* vol. 29, no. 1, 2014.

[33] R. Nader, S. I. I. Ibrahim, and A. H. Al-Hamdani, "Linear and Nonlinear Optical Properties of Anthocyanin Dye from Red Cabbage in Different pH Solutions," *Baghdad Science Journal,* vol. 20, no. 3 (Suppl.), pp. 1131-1131, 2023.

[34] C. Gautier, P. Fichet, D. Menut, J.-L. Lacour, D. L'Hermite, and J. Dubessy, "Study of the double-pulse setup with an orthogonal beam geometry for laser-induced breakdown spectroscopy," *Spectrochimica Acta Part B: Atomic Spectroscopy,* vol. 59, no. 7, pp. 975-986, 2004.

[35] Z. Khan *et al.*, "Laser-Induced Breakdown Spectroscopy (LIBS) for Trace Element Detection: A Review," *Journal of Spectroscopy,* vol. 2022, no. 1, p. 3887038, 2022.

[36] W. Demtröder, *Laser spectroscopy: vol. 2: experimental techniques*. Springer Science & Business Media, 2008.

[37] D. Anglos *et al.*, "Artwork diagnostics: laser induced breakdown spectroscopy (LIBS) and laser induced florescence (LIF) spectroscopy," in *Proceedings of the first international conference on lasers in the conservation of artworks. Heraklion, Greece*, 1995, pp. 113-8.

[38] V. Rai and S. Thakur, "Physics of plasma in laser-induced breakdown spectroscopy," *Laser-induced breakdown spectroscopy,* pp. 83-111, 2007.

[39] J. Ge *et al.*, "An Optical Ultrahigh-Resolution Cross-dispersed Echelle Spectrographwith Adaptive Optics1," *Publications of the Astronomical Society of the Pacific,* vol. 114, no. 798, p. 879, 2002.

[40] D. A. Cremers, L. J. Radziemski, and T. R. Loree, "Spectrochemical analysis of liquids using the laser spark," *Applied spectroscopy,* vol. 38, no. 5, pp. 721-729, 1984.

[41] R. Sattmann, V. Sturm, and R. Noll, "Laser-induced breakdown spectroscopy of steel samples using multiple Q-switch Nd: YAG laser pulses," *Journal of Physics D: Applied Physics,* vol. 28, no. 10, p. 2181, 1995.

[42] V. N. Rai, F.-Y. Yueh, and J. P. Singh, "Study of laser-induced breakdown emission from liquid under double-pulse excitation," *Applied optics,* vol. 42, no. 12, pp. 2094-2101, 2003.

[43] L. St-Onge, V. Detalle, and M. Sabsabi, "Enhanced laser-induced breakdown spectroscopy using the combination of fourth-harmonic and fundamental Nd: YAG laser pulses," *Spectrochimica Acta Part B: Atomic Spectroscopy,* vol. 57, no. 1, pp. 121-135, 2002.

[44] J. Uebbing, J. Brust, W. Sdorra, F. Leis, and K. Niemax, "Reheating of a laser-produced plasma by a second pulse laser," *Applied spectroscopy,* vol. 45, no. 9, pp. 1419-1423, 1991.

[45] X. Pu and N. Cheung, "ArF laser induced plasma spectroscopy of lead ions in aqueous solutions: plume reheating with a second Nd: YAG laser pulse," *Applied spectroscopy,* vol. 57, no. 5, pp. 588-590, 2003.

[46] S. Moncayo *et al.*, "Multi-elemental imaging of paraffin-embedded human samples by laser-induced breakdown spectroscopy," *Spectrochimica Acta Part B: Atomic Spectroscopy,* vol. 133, pp. 40-44, 2017.

[47] B. Busser *et al.*, "Characterization of foreign materials in paraffin-embedded pathological specimens using in situ multi-elemental imaging with laser spectroscopy," *Modern Pathology,* vol. 31, no. 3, pp. 378-384, 2018.

[48] X. Li, H. Yin, Z. Wang, Y. Fu, Z. Li, and W. Ni, "Quantitative carbon analysis in coal by combining data processing and spatial confinement in laser-induced breakdown spectroscopy," *Spectrochimica Acta Part B: Atomic Spectroscopy,* vol. 111, pp. 102-107, 2015.

[49] M. Kasem, J. Gonzalez, R. Russo, and M. Harith, "Effect of the wavelength on laser induced breakdown spectrometric analysis of archaeological bone," *Spectrochimica Acta Part B: Atomic Spectroscopy,* vol. 101, pp. 26-31, 2014.

[50] M. Martinez and M. Baudelet, "Matrix-matched calibration material for zinc analysis of human nails by laser-induced breakdown spectroscopy," *Spectrochimica Acta Part B: Atomic Spectroscopy,* vol. 163, p. 105732, 2020.

[51] S. Hamzaoui, I. Cherni, and N. Jaidene, "The Study of Hair from Men with Androgenetic Alopecia Using the Laser-induced Breakdown Spectroscopy (LIBS) Technique," *Lasers in Engineering (Old City Publishing),* vol. 41, 2018.

[52] Z. Feng *et al.*, "Electrolyte Analysis in Blood Serum by Laser-Induced Breakdown Spectroscopy Using a Portable Laser," *Molecules,* vol. 27, no. 19, p. 6438, 2022. [Online]. Available: https://www.mdpi.com/1420-3049/27/19/6438.

[53] Q. Sun, M. Tran, B. Smith, and J. D. Winefordner, "In-situ evaluation of barrier-cream performance on human skin using laser-induced breakdown spectroscopy," *Contact Dermatitis,* vol. 43, no. 5, pp. 259-263, 2000.